BOSOR4: PROGRAM FOR STRESS, BUCKLING, AND VIBRATION OF COMPLEX SHELLS OF REVOLUTION

David Bushnell

Lockheed Missiles & Space Co., Inc.

INTRODUCTION

A comprehensive computer program, designated BOSOR4, for analysis of the stress, stability and vibration of segmented, ring-stiffened, branched shells of revolution and prismatic shells and panels is described. The program performs large-deflection axisymmetric stress analysis, small-deflection nonsymmetric stress analysis, modal vibration analysis with axisymmetric nonlinear prestress included, and buckling analysis with axisymmetric or nonsymmetric prestress. One of the main advantages of the code is the provision for realistic engineering details such as eccentric load paths, internal supports, arbitrary branching conditions, and a 'library' of wall constructions. The program is based on the finite difference energy method which is very rapidly convergent with increasing numbers of mesh points. Overlay charts and core storage requirements are given for the CDC 6600, IBM 370/165, and UNIVAC 1108/1110 versions of BOSOR4. Several examples are included to demonstrate the scope and practicality of the program. Some hints are given to help the user generate appropriate analytical models. An appendix contains the user's manual for BOSOR4.

Table 1 shows the characteristics and status of BOSOR4. The program is currently in widespread use and is maintained by the developer. Notices of any bugs found are promptly circulated to all known users and data centers that have acquired BOSOR4.

The BOSOR4 program was developed in response to the need for a tool which would help the engineer to design practical shell structures. An important class of such shell structures includes segmented, ring-stiffened branched shells of revolution. These shells may have various meridional geometries, wall constructions, boundary conditions, ring reinforcements, and types of loading, including thermal loading. An example is shown in Fig. 1. The meridian of the shell of revolution consists of six segments with various geometries and wall constructions. The first segment (nearest the bottom, end "A") is a monocoque ogive with variable thickness; the second is a conical shell with three layers of

Table 1 BOSOR4 at a Glance

Keywords: shells, stress, buckling, vibration, nonlinear, elastic, shells of revolution, ring-stiffened, branched, composites, discrete model
Purpose: To perform stress, buckling, and modal vibration analyses of ring-stiffened, branched shells of revolution loaded either axisymmetrically or nonsymmetrically. Complex wall construction permitted.
Date: 1972; most recent update 1975
Developer: David Bushnell, 52-33/205
Lockheed Missiles & Space Co., Inc.
3251 Hanover Street
Palo Alto, Ca. 94304
Tel: (415) 493-4411, X45491 or 43851
Method: Finite difference energy minimization; Fourier superposition in circumferential variable; Newton method for solution of nonlinear axisymmetric problem; inverse power iteration with spectral shifts for eigenvalue extraction; Lagrange multipliers for constraint conditions; thin shell theory.
Restrictions: 1500 degrees of freedom (d.o.f.) in nonaxisymmetric problems; 1000 d.o.f. in axisymmetric prebuckling stress analysis; Maximum of 20 Fourier harmonics per case; Knockdown factors for imperfections not included; Radius/thickness should be greater than about 10.
Language: FORTRAN IV
Documentation: BOSOR4 User's Manual [1] and about 10 journal articles with numerous examples.
Input: Preprocessor written by SKD Enterprise, 9138 Barberry Lane, Hickory Hills, Illinois 60457 for free-field input. Required for input are shell segment geometries, ring geometries, number of mesh points, ranges and increments of circumferential wave numbers, load and temperature distributions, shell wall construction details, and constraint conditions.
Output: Stress resultants or extreme fiber stresses, buckling loads, vibration frequencies; list and plots.
Hardware: UNIVAC 1108/110, CDC 6600/7600, IBM 360/370; SC4020 and CALCOMP plotters
Usage: About 100 institutions have obtained BOSOR4. It is currently being used on a daily basis by many of them.
Run Time: Typically a job will require 1-10 minutes of computer time.
Availability: CDC and UNIVAC versions from developer (see above); IBM version from Prof. Victor Weingarten, Dept. of Civil Eng., Univ. of Southern Calif., University Park, Los Angeles, Calif. 90007; Price: $300. In addition to the Software Series participating networks mentioned in this volume, BOSOR4 may be run through the following data centers:

McDonnell-Douglas Automation, Huntington Beach, Calif.
Control Data Corp., Rockville, Md.
Westinghouse Telecomputer, Pittsburgh, Penna.
Information System Design, Oakland, Calif.
Boeing Computer Service, Seattle, Wash.

temperature-dependent, orthotropic material; the third is a layered, fiber-wound cylinder; the fourth is a toroidal segment with eccentric rings and stringers; the fifth is a spherical segment with eccentric rings and stringers; and the sixth is a flat plate with sandwich construction and eccentric meridional stiffeners. The reference surface is indicated by the dark dash-dot line. It is seen that the meridian of the composite shell structure is discontinuous between the first and second segments, the second and third segments, and the third and fourth segments. In the analysis these discontinuities are accounted for. The shell is supported at the end "A" by a ring which is restrained as shown: axial and radial displacements u* and w* are not permitted at the point "A", which is located a specified distance from the beginning of the reference surface. In the analysis of actual shell structures it is important that support points, junctures, and ring reinforcements be accurately modeled. Seemingly insignificant parameters sometimes have a large effect on the stress, buckling loads, and vibration frequencies. The shell is reinforced by 6 rings of rectangular cross section, the centroids of which are shown in the figure. These rings are treated as discrete elastic structures in the analysis. The shell is submitted to uniform external pressure (not shown), line loads applied at the first and second rings, and the thermal environment depicted on the second segment.

Figures 2 and 3 show computer-generated plots from a linear buckling analysis and free vibration analysis. Normal displacement components w of the modes are shown for the lowest three eigenvalues corresponding to circumferential harmonics n = 4, 6, 8, 10, 12 and 14. The regions of the six shell segments are indicated in Fig. 2. In the buckling analysis the uniform pressure is the eigenvalue parameter, all other mechanical and thermal loads being held fixed. In the vibration analysis the external pressure is 40 psi and all loads are held fixed. Calculation of the 18 eigenvalues requires 8 min for the buckling analysis and 6 min for the vibration analysis. Computations were performed on the UNIVAC 1108, in double precision. There are 460 degrees of freedom in the discrete model.

BOSOR4 has been in use at Lockheed and elsewhere since 1972. During that time it has been used in several projects, some of them involving rather complex shells of revolution. An example is shown in Fig. 4, which depicts a somewhat idealized model of a cryogenic cooler. The axisymmetric structure consists of a series of fiberglas tubes from which are suspended two axisymmetric cryogenic tanks. The object of this study was to determine the natural frequencies of the cooler corresponding to beam-type modes (n=1 circumferential wave). The discretized model is shown in Fig. 5 and the first four vibration modes in Fig. 6.

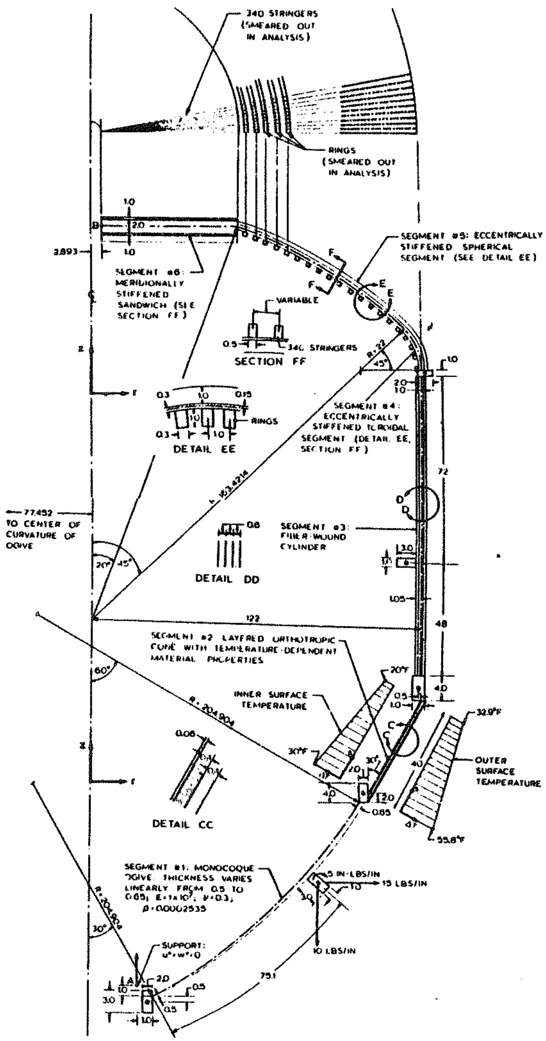

Fig. 1 Segmented composite shell for analysis by BOSOR4

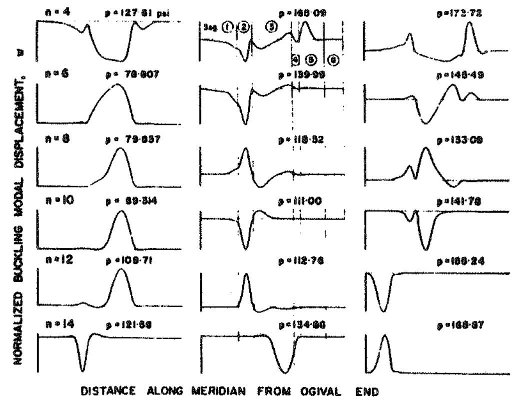

Fig. 2 w-components of eigenvectors for linear buckling analysis of externally pressurized six-segment shell shown in Fig. 1

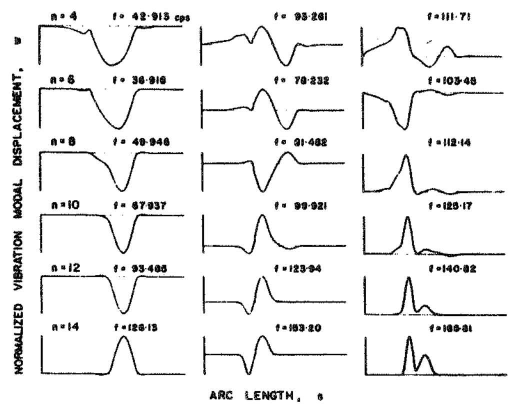

Fig. 3 w-components of eigenvectors for free vibration analysis of six-segment shell shown in Fig. 1

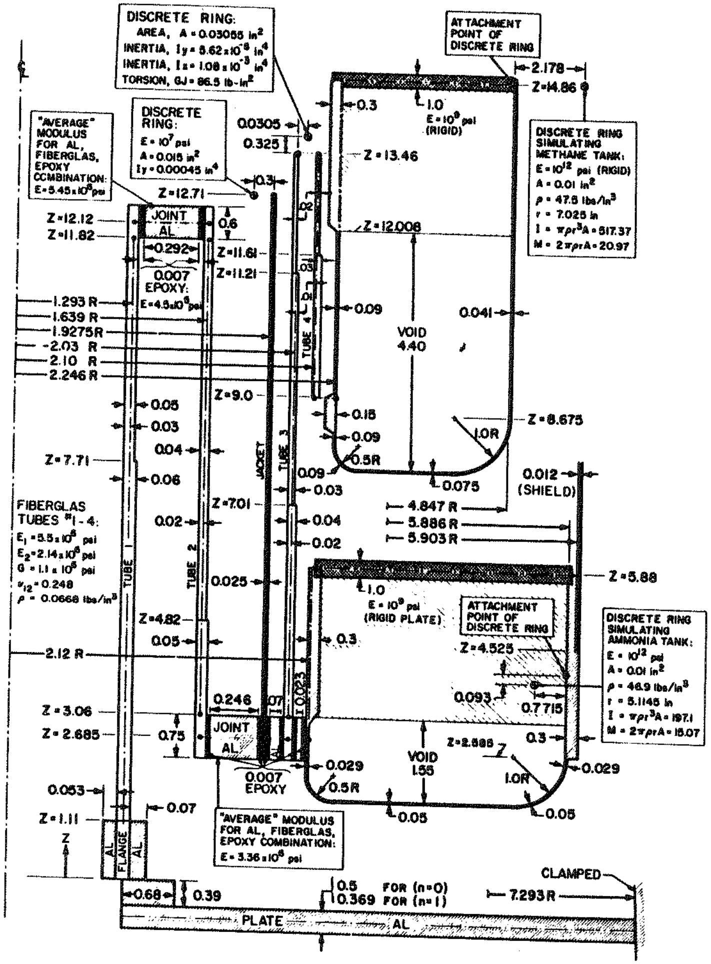

Fig. 4 Cryogenic cooler model for BOSOR4

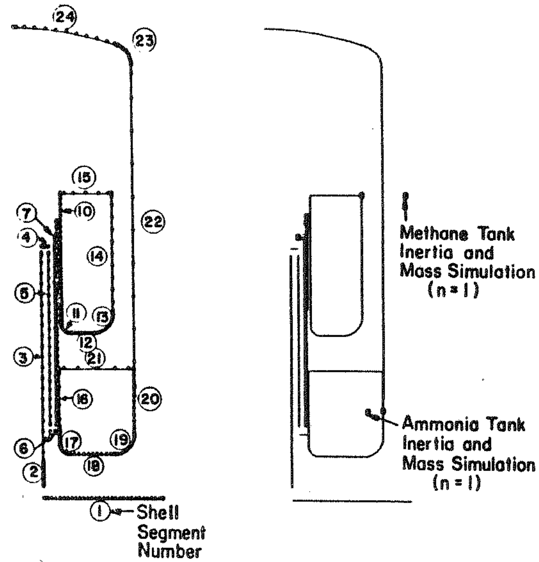

Fig. 5 BOSOR4 model for lateral (n=1) vibration, showing shell segments, mesh points, and locations of centroids of discrete rings which simulate mass and moment of inertia of methane and ammonia tanks

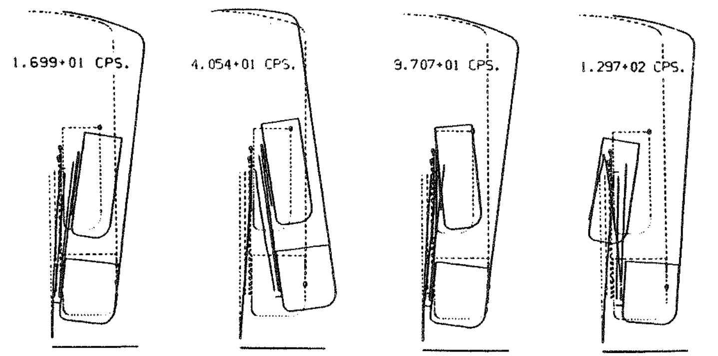

Fig. 6 First four lateral (n=1) vibration modes with BOSOR4 model

SCOPE OF THE BOSOR4 COMPUTER PROGRAM

The BOSOR4 code performs stress, stability, and vibration analyses of segmented, branched, ring-stiffened, elastic shells of revolution with various wall constructions. Figure 7 shows some examples of branched structures which can be handled by BOSOR4. Figure 7a represents part of a multiple-stage rocket treated as a shell of seven segments; Fig. 7b represents part of a ring-stiffened cylinder in which the ring is treated as two shell segments branching from the cylinder; Fig. 7c shows the same ring-stiffened cylinder, but with the ring treated as 'discrete', that is the ring cross section can rotate and translate but not deform, as it can in the model shown in Fig. 7b. Figures 7d-f represent branched prismatic shell structures, which can be treated as shells of revolution with very large mean circumferential radii of curvature, as described in [2] and later in this paper.

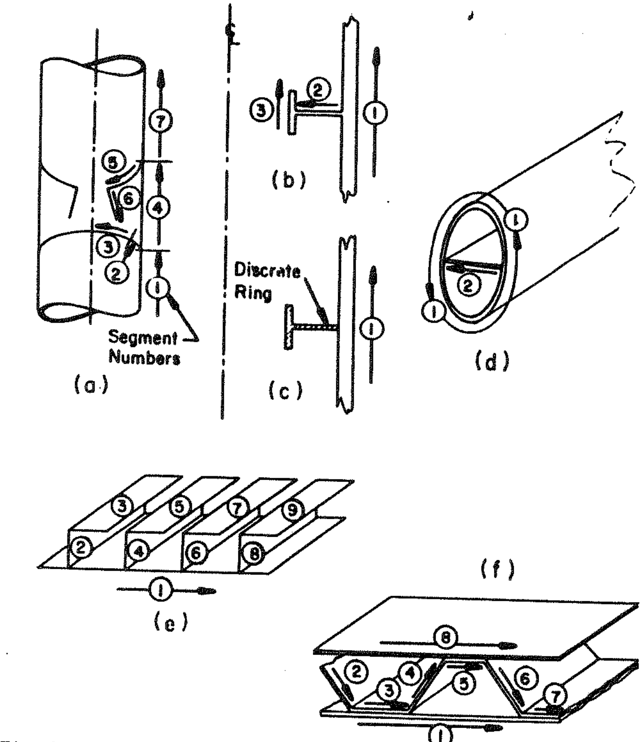

Fig. 7 Examples of branched structures which can be analyzed with BOSOR4

The program is very general with respect to geometry of meridian, shell-wall design, edge conditions, and loading. It has been thoroughly checked out by comparisons with other known solutions and tests and by extensive use at a number of different institutions over the past three years. The BOSOR4 capability is summarized in Table 2. The code represents three distinct analyses:

1. A nonlinear stress analysis for axisymmetric behavior of axisymmetric shell systems (large deflections, elastic)
2. A linear stress analysis for axisymmetric and nonsymmetric behavior of axisymmetric shell systems submitted to axisymmetric and nonsymmetric loads
3. An eigenvalue analysis in which the eigenvalues represent buckling loads or vibration frequencies of axisymmetric shell systems submitted to axisymmetric loads. (Eigenvectors may correspond to axisymmetric or nonsymmetric modes.)

BOSOR4 has an additional branch corresponding to buckling of nonsymmetrically loaded shells of revolution. However, this branch is really a combination of the second and third analyses just listed.

Table 2 BOSOR4 Capability Summary

Type of analysis	Shell geometry	Wall construction	Loading
Nonlinear axisymmetric stress Linear symmetric or nonsymmetric stress Stability with linear symmetric or nonsymmetric prestress or with nonlinear symmetric prestress Vibration with nonlinear prestress analysis Variable mesh point spacing within each segment	Multiple-segment shells, each segment with its own wall construction, geometry, and loading Cylinder, cone, spherical, ogival, toroidal, ellipsoidal, etc. General meridional shape; point-by-point input Axial and radial discontinuities in shell meridian Arbitrary choice of reference surface General edge conditions Branched shells Prismatic shells and composite built-up panels	Monocoque, variable or constant thickness Skew-stiffened shells Fiber-wound shells Layered orthotropic shells Corrugated, with or without skin Layered orthotropic with temperature-dependent material properties Any of above wall types reinforced by stringers and/or rings treated as "smeared out" Any of above wall types further reinforced by rings treated as discrete Wall properties variable along meridian	Axisymmetric or nonsymmetric thermal and/or mechanical line loads and moments Axisymmetric or nonsymmetric thermal and/or mechanical distributed loads Proportional loading Non-proportional loading

In the BOSOR4 code, the user chooses the type of analysis to be performed by means of a control integer INDIC:

INDIC = -2 Stability determinant calculated for given circumferential wave number N for increasing loads until it changes sign. Nonlinear prebuckling effects included. INDIC then changed automatically to -1 and calculations proceed as if INDIC has always been -1.

INDIC = -1 Buckling load and corresponding wave number N determined, including nonlinear prebuckling effects. N corresponding to local minimum critical load $L_{cr}(N)$ is automatically sought.

INDIC = 0 Axisymmetric stresses and displacements calculated for a sequence of stepwise increasing loads from some starting value to some maximum value, including nonlinear effects. Axisymmetric collapse loads can be calculated.

INDIC = 1 Buckling loads calculated with nonlinear bending theory for a fixed load. Buckling loads calculated for a range of circumferential wave numbers. Several buckling loads for each wave number can be calculated.

INDIC = 2 Vibration frequencies and mode shapes calculated, including the effects of prestress obtained from axisymmetric nonlinear analysis. Several frequencies and modes can be calculated for each circumferential wave number.

INDIC = 3 Nonsymmetric or symmetric stresses and displacements calculated for a range of circumferential wave numbers. Linear theory used. Results for each harmonic are automatically superposed. Fourier series for nonsymmetric loads are automatically computed or may be provided by user.

INDIC = 4 Buckling loads calculated for nonsymmetrically loaded shells. Prebuckled state obtained from linear theory (INDIC = 3) or read in from cards. 'Worst' meridional prestress distribution (such as distribution involving maximum negative meridional or hoop prestress resultant) chosen by user, and this particular distribution is assumed to be axisymmetric in the stability analysis, which is the same as that for the branch INDIC = 1.

The variety of buckling analyses (INDIC = -2, -1, 1, and 4) is to permit the user to approach a given problem in a number of different ways. There are cases for which an INDIC = -1 analysis, for example, will not work. The user can then resort to an INDIC = -2 analysis, which requires more computer time, but which is generally more reliable. Buckling of a shallow spherical cap under external pressure is an example. In an INDIC = -1 analysis of the cap, the program generates a sequence of loads that ordinarily should converge to the lowest buckling load, with nonlinear prebuckling effects included. Depending on the cap geometry and the user-provided initial pressure, however, one of the loads in the sequence may exceed the axisymmetric collapse pressure of the cap. This phenomenon can occur if the bifurcation buckling loads are just slightly smaller than the axisymmetric collapse loads. The user can obtain a solution with use of INDIC = -2, in which the bifurcation load is approached from below in a 'gradual' manner.

The branch INDIC = 1 is provided because it is sometimes desirable to know several buckling eigenvalues for each circumferential wave number, N, and because there may exist more than one minimum in the critical load vs N-space. This is especially true for composite shell structures with many segments and load types. Such a structure can buckle in many different ways. The designer may have to eliminate several possible failure modes, not just the one corresponding to the lowest pressure, for example. The INDIC = 4 branch is provided for two reasons: The user can calculate buckling under nonsymmetric loads without having to make two separate runs, an INDIC = 3 run and an INDIC = 1 run. In addition, this branch permits the user to bypass the prebuckling analysis and read prebuckling stress distributions and rotations directly from cards. This second feature is very useful for the treatment of composite branched panels under uniaxial or biaxial compression.

The BOSOR4 program, although applicable to shells of revolution, can be used for the buckling analysis of composite, branched panels by means of a 'trick' described in detail in Ref [2]. This 'trick' permits the analysis of any prismatic shell structure that is simply-supported at particular stations along the length. Any boundary conditions can be used along generators. In [2] many examples are given, including nonuniformly loaded cylinders, noncircular cylinders, corrugated panels, and cylinders with stringers treated as discrete. This paper gives other examples.

ANALYSIS METHOD

The assumptions upon which the BOSOR4 code is based are:

1. The wall material is elastic.
2. Thin shell theory holds; i.e. normals to the undeformed surface remain normal and undeformed.

3. The structure is axisymmetric, and in vibration analysis and nonlinear stress analysis the loads and prebuckling or prestress deformations are axisymmetric.

4. The axisymmetric prebuckling deflections in the nonlinear theory (INDIC = 0, -1, 2), while considered finite, are moderate; i.e. the square of the meridional rotation can be neglected compared with unity.

5. In the calculation of displacement and stresses in nonsymmetrically loaded shells (INDIC = 3), linear theory is used. This branch of the program is based on standard small-deflection analysis.

6. A typical cross sectional dimension of a discrete ring stiffener is small compared with the radius of the ring.

7. The cross sections of the discrete rings remain undeformed as the structure deforms, and the rotation about the ring centroid is equal to the rotation of the shell meridian at the attachment point of the ring (except, of course, if the ring is treated as a flexible shell branch).

8. The discrete ring centroids coincide with their shear centers.

9. If meridional stiffeners are present, they are numerous enough to include in the analysis by an averaging or 'smearing' of their properties over any parallel circle of the shell structure. Meridional stiffeners can be treated as discrete through the 'trick' described in Ref. [2].

The analysis is based on energy minimization with constraint conditions. The total energy of the system includes strain energy of the shell segments and discrete rings, potential energy of the applied line loads and pressures, and kinetic energy of the shell segments and discrete rings. The constraint conditions arise from displacement conditions at the boundaries of the structure, displacement conditions that may be prescribed anywhere within the structure, and at junctures between segments. The constraint conditions are introduced into the energy function by means of Lagrange multipliers.

These components of energy and constraint conditions are initially integro – differential forms. The circumferential dependence is eliminated by separation of variables. Displacements and meridional derivatives of displacements are then written in terms of the shell reference surface components u_i, v_i and w_i at the finite-difference mesh points and Lagrange multipliers λ_i. integration is performed simply by multiplication of the energy per unit length of meridian by the length of the 'finite difference element', to be described below.

In the nonlinear axisymmetric stress analysis the energy expression has terms linear, quadratic, cubic, and quartic in the dependent variables u_i and w_i. The cubic and quartic energy terms arise from the rotation-squared terms that appear in the expression for reference surface meridional strain and in the constraint conditions. Energy minimization leads to a set of nonlinear algebraic equations that are solved by the Newton-Raphson method. Stress and moment resultants are calculated in a straightforward manner from the mesh-point displacement components through the constitutive equations and the kinematic relations.

The results from the nonlinear axisymmetric or linear nonsymmetric stress analysis are used in the eigenvalue analyses for buckling and vibration. The 'prebuckling' or 'prestress' meridional and circumferential stress resultants N_{10} and N_{20} and the meridional rotation χ_o appear as known variable coefficients in the energy expressions that govern buckling and vibration. These expressions are homogeneous quadratic forms. The values of a parameter (load or frequency) that render the quadratic forms stationary with respect to infinitesimal variations of the dependent variables represent buckling loads or natural frequencies. These eigenvalues are calculated from a set of linear homogeneous equations. More will be written about the bifurcation buckling eigenvalue problems in the following paragraphs.

Details of the analysis are given in [1, 3 and 4]. Only two aspects will be described here: the finite difference element and the stability eigenvalue problem.

The 'Finite Difference' Element

BOSOR4 is based on the finite difference energy method. This method is described in detail and compared with the finite element method in [5]. Figure 8 shows a typical shell segment meridian with finite difference mesh points. The 'u' and 'v' points are located halfway between adjacent 'w' points. The energy contains up to first derivatives in u and v and up to second derivatives in w. Hence, the shell energy density evaluated at the point labeled E (center of the length ℓ) involves the seven points w_{i-1} through w_{i+1}. The energy per unit circumferential length is simply the energy per unit area multiplied by the length of the finite difference element ℓ, which is the arc length of the reference surface between two adjacent u or v points. In Ref. [5] it is shown that this formulation yields a 7 x 7 stiffness matrix corresponding to a constant strain, constant curvature change finite element that is incompatible in normal displacement and rotation at its boundaries but that in general gives very rapidly convergent results with increasing density of nodal points. Note that two of the w points lie outside of the element. If the mesh spacing is

Fig. 8 Finite difference discretization: the 'finite difference element'

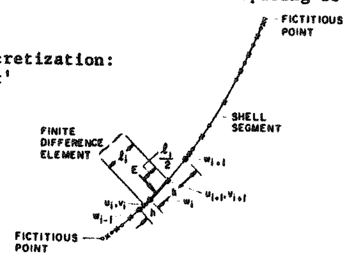

constant, the algebraic equations obtained by minimization of the energy with respect to nodal degrees of freedom can be shown to be equivalent to the Euler equations of the variational problem in finite form. Further description and proofs are given in Ref. [5].

Figures 9 and 10 show rates of convergence with increasing nodal point density for a poorly conditioned problem — a stress analysis of a thin, nonsymmetrically loaded hemisphere with a free edge. The finite element results were obtained by programming various kinds of finite elements into BOSOR4. The computer time for computation of the stiffness matrix K_1 is shown in Fig. 10. A much smaller time for computation of the finite difference K_1 is required because there are fewer calculations for each Gaussian integration point and because there is only one Gaussian point per finite difference element. Other comparisons of rate of convergence with the two methods used in BOSOR4 are shown for buckling and vibration problems in Ref. [5].

Formulation of the Stability Problem

The bifurcation buckling problem represents perhaps the most difficult of the three types of analyses performed by BOSOR4. It is practical to consider bifurcation buckling of complex, ring stiffened shell structures under various systems of loads, some of which are considered to be known and constant, or 'fixed' and some of which are considered to be unknown eigenvalue parameters, or 'variable'.

The notion of 'fixed' and 'variable' systems of loads not only permits the analysis of structures submitted to nonproportionally varying loads, but also helps in the formulation of a sequence of simple or 'classical' eigenvalue problems for the solution of problems governed by 'nonclassical' eigenvalue problems. An example is a shallow spherical cap under external pressure. Very shallow caps fail by nonlinear collapse, or snap-through buckling, not by bifurcation buckling. Deep spherical caps fail by bifurcation buckling in which nonlinearities in prebuckling behavior are not particularly important. There is a range of cap geometries for which bifurcation buckling is the mode of failure and for which the critical pressures are much affected by nonlinearities in prebuckling behavior. The analysis of this intermediate class of spherical caps is simplified by the concept of 'fixed' and 'variable' pressure.

Figure 11 shows the load deflection curve of a shallow cap in this intermediate range. Nonlinear axisymmetric collapse (p_{nl}), linear bifurcation (p_{lb}), and nonlinear bifurcation (p_{nb}) loads are shown. The purpose of the analysis referred to in this section is to determine the pressure p_{nb}. It is useful to consider the pressure p_{nb} as composed of two parts

$$p_{nb} = p^f + p^v$$

in which p^f denotes a known or 'fixed' quantity, and p^v denotes an undetermined or 'variable' quantity. The fixed portion p^f is an

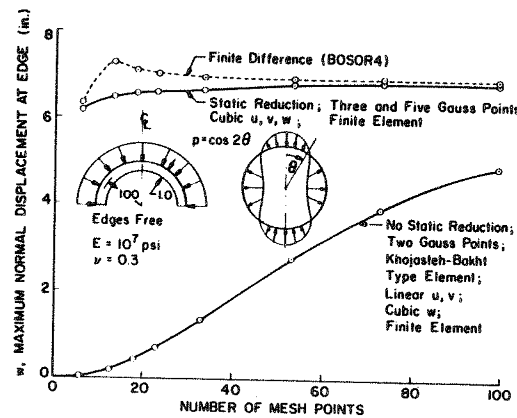

Fig. 9 Normal displacement at free edge of hemisphere with nonuniform pressure $p(s,\theta) = p_o \cos 2\theta$

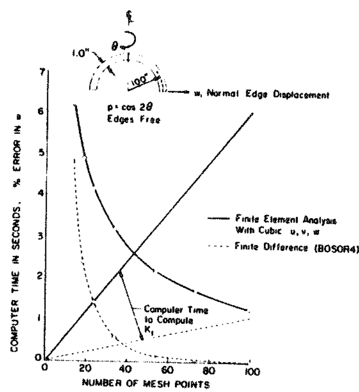

Fig. 10 Computer times to form stiffness matrix K_1 and rates of convergence of normal edge displacement for free hemisphere with nonuniform pressure $p(s,\theta) = p_o \cos 2\theta$

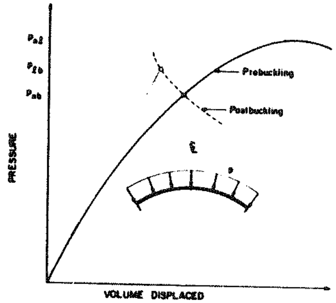

Fig. 11 Load deflection curves for shallow spherical cap, showing bifurcation points from linear prebuckling curve ($p_{\ell b}$) and nonlinear prebuckling curve (p_{nb})

initial guess or represents the results of a previous iteration. The variable portion p^v is the remainder, which can be determined from an eigenvalue problem, as will be described. It is clear from Fig. 11 that if p^f is fairly close to p_{nb} the behavior in the range $p = p^f \pm p^v$ is reasonably linear. Thus, the eigenvalue p_{nb} can be calculated by means of a sequence of eigenvalue problems through which ever and ever smaller values p^v are determined and added to the known results p^f from the previous iterations. As the BOSOR4 computer program is written the initial guess p^f need not be close to the solution p_{nb}.

In the bifurcation stability analysis it is necessary to develop two matrices corresponding to the eigenvalue problem

$$K_1(n)x_n + \lambda_n K_2(n)x_n = 0. \qquad (1)$$

In Eq. (1) $K_1(n)$ is the stiffness matrix of the shell as loaded by the fixed load system p^f; $K_2(n)$ is the load-geometric matrix corresponding to the prestress increment caused by the loading increment p^v; λ_n is the eigenvalue; x_n is the eigenvector; and n is the number of full circumferential waves. Eigenvalues are extracted by inverse power iterations with spectral shifts. Further details of the theory are given in [6], including the treatment of the discrete ring stiffeners and constraint conditions.

IMPERFECTION SENSITIVITY IN BUCKLING ANALYSES

It is well known that the load-carrying capability of thin shells is in many cases sensitive to initial imperfections of the geometry of the shell wall. The question so often asked by the analyst is: given the idealized structure and loading, and given the means by which to determine the collapse or bifurcation buckling loads, what "knockdown" factor should be applied to assure a reasonable factor of safety for the actual imperfect structure?

In Fig. 15 is an example of a shell-load system which exhibits load carrying capability considerably greater than that corresponding to the lowest bifurcation eigenvalue. Postbuckling stability is also exhibited by columns and flat plates. On the other hand, it is well known that the critical loads of axially compressed cylindrical shells and externally pressurized spherical shells are extremely sensitive to imperfections less than one wall thick in magnitude. These highly symmetrical systems are very sensitive to imperfections because many different buckling modes are associated with the same eigenvalue, the structure is uniformly compressed in a membrane state, and the buckling modes have many small waves. Very small local imperfections will tend to trigger premature failure. The buckling loads of most practical shell structures are somewhat sensitive to imperfections, but not this sensitive. How much so is a very important question. BOSOR4 does not calculate "knock down" factors to account for imperfections. With BOSOR4 the analyst can calculate buckling loads of shells with arbitrary axisymmetric imperfections. The BOSOR4 user is urged to read the brief survey of imperfection sensitivity theory given in [7] and to consult the references given there.

BOSOR4 PROGRAM ORGANIZATION

The BOSOR4 program consists of a main program MAIN and six overlays called READIT, PRE, ARRAYS, BUCKLE, MODE1, AND PLOT1. Figure 12 gives the core storage in decimal words required for the Univac 1108, IBM 370, and CDC 6600 versions of BOSOR4. The Univac 1108 and IBM 370 versions are written in double precision FORTRAN IV; the CDC version is written in single precision FORTRAN IV.

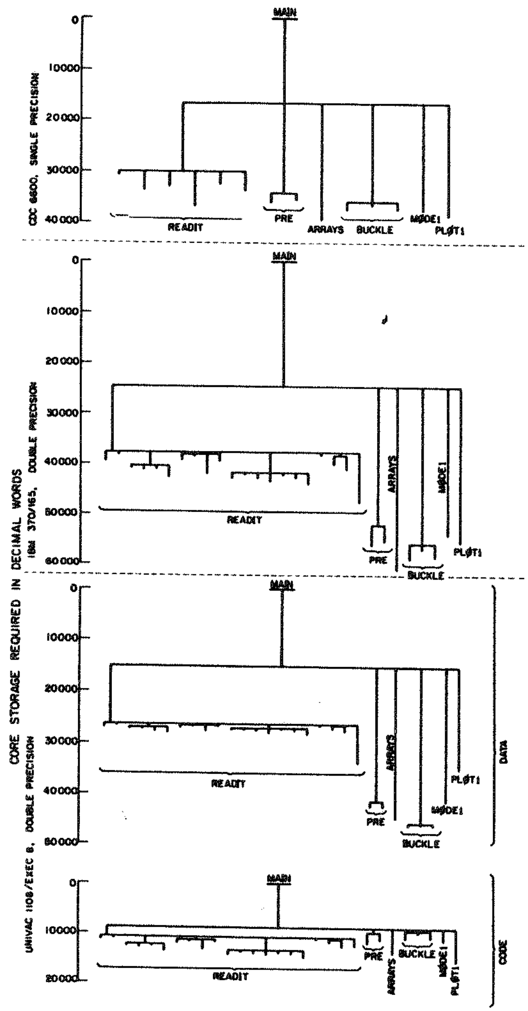

Fig. 12 BOSOR4 core storage requirements

SAMPLE DESIGN PROBLEMS FOR WHICH BOSOR4 HAS BEEN USED AND COMPARISON WITH TESTS

A complex design that BOSOR4 was used on is shown in Fig. 4. Other examples corresponding to various analysis branches (INDIC) are given in this section.

Nonlinear Stress Analysis (INDIC = 0)

Figure 13 shows part of an internally pressurized elliptical tank which has been thickened locally near the equator for welding. The engineering drawings called for an elliptically shaped inner surface with the thickness varying as shown. The maximum stress occurs at the outer fiber at point C because there is considerable local bending there due to the rather sudden change in direction, or eccentricity, of the load path in the short segment ACB. The nonlinear theory gives lower stresses than the linear theory because the meridional tension causes the tank to change shape in such a way as to decrease the local excursion of the load path, thereby decreasing the effective bending moment acting at point C. The tank had been built and a linear analysis performed. The user of the tank wanted to know if it would withstand a somewhat higher internal pressure than that for which it had originally been designed. The lower stress predicted with nonlinear theory gave him enough margin of safety to avoid the necessity of redesign.

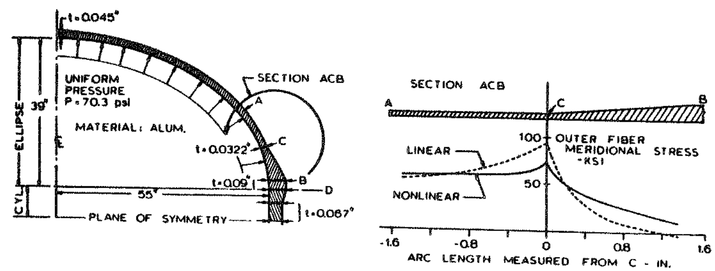

Fig. 13 Linear and nonlinear analysis of internally pressurized elliptical tank

T-ring Modeled as Branched Shell (INDIC = 0)

Figure 14 shows the discretized model and buckling loads predicted for a range of circumferential waves N. BOSOR4 gives two minima in the range $2 \geq N \geq 16$. The minimum at N = 2 is a mode in which the cross section does not deform, i.e. the ring ovalization mode. Buckling pressures calculated for this mode are very close to those computed from the well known formula $q_{cr} = EI(N^2 - 1)/r_c^3$, in which qcr is the critical line load in lb/in. (pressure integrated in the direction of segment 1), EI is the bending rigidity of the ring, and r_c is the radius to the ring centroidal axis. The minimum at about N = 11 corresponds to buckling of the web. In a test the web crippled at about 1500 psi. The N = 2 mode was not observed because the ring was held in a mandrel that prevented the unlimited growth of this mode. Approximately 20 sec of UNIVAC 1108 CPU time were required for this case.

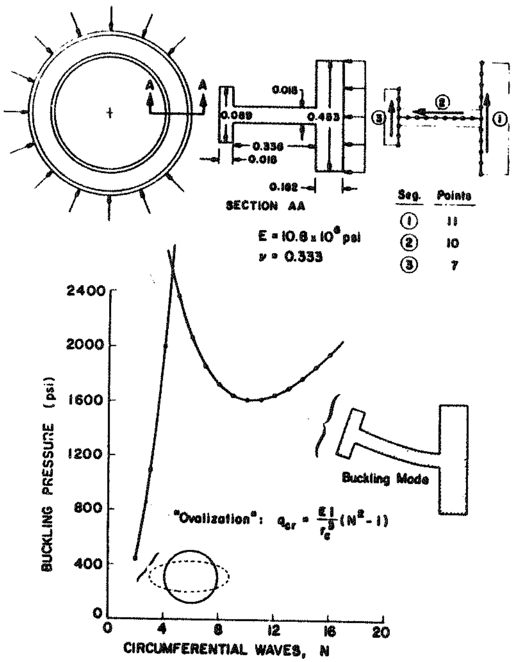

Fig. 14 Buckling of ring treated as branched shell

Nonlinear Bifurcation Buckling (INDIC = -2 and -1)

Point-loaded spherical caps were tested by Penning and Thurston in 1965 [8]. A configuration and predicted and experimental load-deflection curves with bifurcation points are shown in Fig. 15. This system is stable at and beyond the bifurcation points shown.

Figure 16 depicts a short section of the generator of a cylinder stiffened by external corrugations. The corrugations are cut away in the neighborhood of a field joint ring to allow for bolting of the two mating flanges of the ring. The cylinder is axially compressed. Far away from the field joint the axial resultant acts through the centroid of the corrugation-skin combination. In the neighborhood of the field joint the load path moves radially inward, effectively causing an axisymmetric dimple. As the axial compression is increased, hoop compressive stresses build up in the regions reinforced by doublers. Slight asymmetry of the assembly causes the ring to roll over axisymmetrically, which generates higher compressive hoop stresses above the ring and eventually leads to buckling there with many small waves around the circumference of the cylinder. Figure 17 shows the actual failure, which agrees with the BOSOR4 prediction.

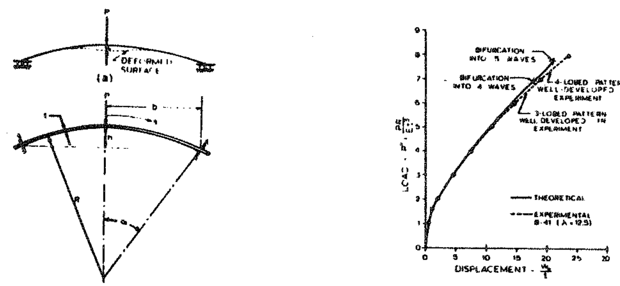

Fig. 15 Point-loaded spherical cap and load-deflection curves obtained from test and from BOSOR4

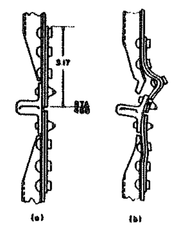

Fig. 16 Field joint geometry and buckle under axial load

Fig. 17 Failure as seen from inside the corrugated cylinder

Nonsymmetric Linear Stress Analysis (INDIC = 3)

Figure 18 gives thermal stresses in a cylinder configured and heated nonsymmetrically as shown. The test results are from [9]. Twenty Fourier harmonics were used for representation of the circumferential temperature distribution and calculation of the stress.

Buckling Under Nonsymmetric Loading (INDIC = 4)

Figures 19 and 20 show the model and results. Figure 19 gives the observed temperature rise distribution at buckling as reported in [10]. Figure 20 shows the predicted prebuckling stress and displacement distributions and the lowest three eigenvalues and eigenvectors corresponding to 20 circumferential waves. The eigenvalues denote a factor to be multiplied by the prebuckling temperature rise distribution at buckling in the test. Twenty Fourier harmonics were used for the prebuckling analysis. The model consists of 309 degrees of freedom. A total of 74 sec of CPU time on the UNIVAC 1108 were required for execution of the case.

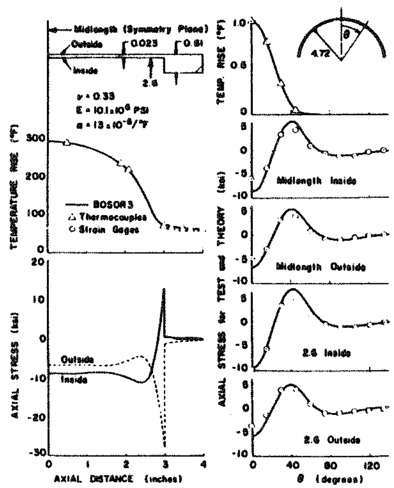

Fig. 18 Comparison of test and theory for thermal stress in nonsymmetrically heated cylinder

Fig. 19 Conical shell heated along axial strip

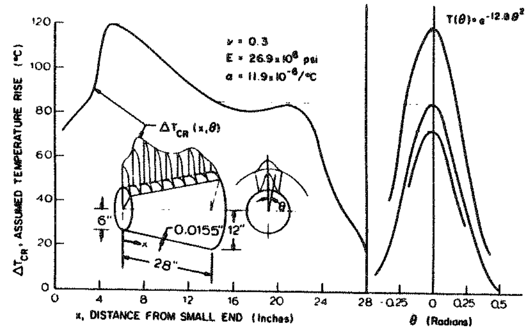

Fig. 20 Prebuckling state of non-axisymmetrically heated cone and buckling modes

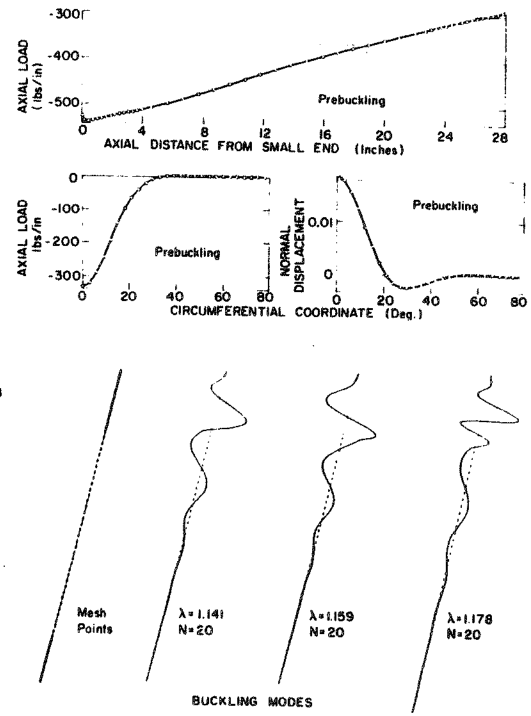

Modal Vibration (INDIC = 2)

Figures 21 and 22 show the geometry and some natural vibration modes of an aluminum ring stiffened cylinder supported by steel end plates. The cylinder was tested by Hayek and Pallett [11] and a previous analysis was performed by Harari and Baron [12]. The experimental results, analytical results from BOSOR4 with eight different models, and analytical results from [12] are given in Table 3.

One of the most important points to be made in regard to Table 3 is that an approximate analysis can by fortuitous coincidence yield very good results because of counteracting errors. Take the bottom row of Table 3, for example. The relatively crude model in which the rings are treated as discrete and the end plates are omitted (modeled as simple supports--v and w restrained, u and rotation free) leads by chance to a very good prediction (2800 cps) of the experimental result (2802 cps). However, the stiffness of each discrete ring is overestimated because its cross section is not permitted to deform. If each ring is treated as a shell segment with no other changes made in the model, a new frequency of 2663 cps is obtained. This branched model is labeled (1) in Fig. 21b. If an additional refinement is made by the addition of the end plates, frequencies of 2682 or 2724 cps are obtained, depending on the degree of constraint assumed to exist between the end plates and the cylinder. These models are too flexible, however, because axial bending of the cylinder wall is permitted along the 0.375 in. lengths corresponding to the regions of intersection of cylinder and rings. If the cylinder is treated as consisting of six segments with 0.375 in. gaps at the areas where the rings and cylinder intersect, and if the material in each gap is treated as a discrete ring with undeformable cross section, the frequencies of 2750 or 2782 or 2833 cps are calculated, depending on whether the end plates are included and, if they are, on the degree of constraint assumed to exist between them and the cylinder. This segmented cylinder model is labeled (2) in Fig. 21b. The predicted vibration mode shapes with n = 6, m = 3 for all of the models are given in Fig. 22. The test frequency of 2802 cps is bracketed by the results from the various models. Notice that for other modes the test frequencies are less well predicted by the cruder discrete ring model but that they are still bracketed (with the exception of n = 5, m = 1) by use of the full range of models as just described. The case n = 6, m = 1 is an example. In the n = 1 case it is important to include the end plates in order to obtain an accurate prediction of the fundamental beam bending mode of the entire free-free cylinder end plate system. This mode is depicted in Fig. 22.

During the study of a particular structure the analyst should set up various models in order to obtain upper and lower bounds on the behavior if possible. Because of imperfections, it is difficult to obtain a lower bound for buckling loads. However, since vibration frequencies and modes are not sensitive to imperfections, vibration test results can usually be regarded as reliable and can therefore be used to determine which models best simulate the actual behavior.

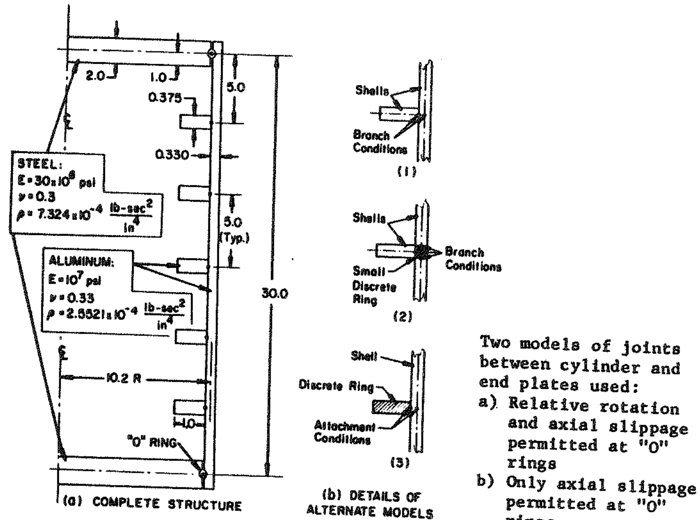

Fig. 21 (a) Geometry of ring stiffened cylinder tested by Hayek and Pallet. (b) Various models of the rings

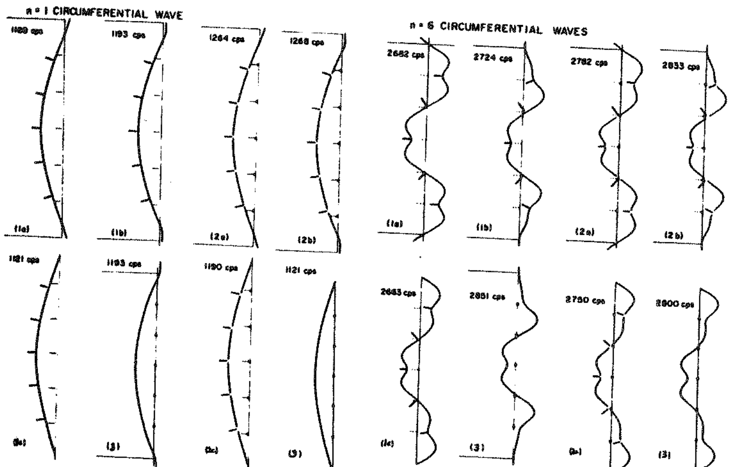

Fig. 22 Vibration modes corresponding to one and six circumferential waves

Table 3 Natural Frequencies for Various Models of Ring-Stiffened Cylinder

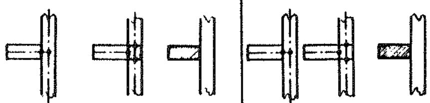

Circ. Waves n	Axial Waves m	Test[a] Results	End Plates Included: Rings Are Shell Branches: Cylinder Is One Segment A[c]	End Plates Included: Rings Are Shell Branches: Cylinder Is One Segment B[d]	End Plates Included: Rings Are Shell Branches: Cylinder Is Six Segments[b] A	End Plates Included: Rings Are Shell Branches: Cylinder Is Six Segments[b] B	End Plates Included: Discrete Rings B	End Plates Omitted: Rings Treated As Shell Branches, Cylinder Segments: One	End Plates Omitted: Rings Treated As Shell Branches, Cylinder Segments: Six	End Plates Omitted: Discrete Rings	Harari & Baron: Discrete Rings	Harari & Baron: Smeared Rings
								Cylinder is Simply			Supported	
1	r.b.[e]	-	0	0	0	0	0	0	0			
1	r.b.[f]	-	0	0	0	0	0	0	0			
1	p.a.	?	0	67	0	69	67	--	--			
1	p.s.[g]	?	0	70	0	73	70	--	--			
1	1	1232	1189	1193	1264	1268	1193	1121	1190	1121	1124	1133
1	u[h]	?	1714	1714	1819	1819	1716	1738	1848	1740	1743	
1	2	?	2189	2198	2301	2313	2199	2175	2282	2177	2183	
1	3	?	2653	2669	2763	2783	2672	2654	2759	2656	2663	
1	4	2870	2863	2887	2962	2991	2890		2960	2868	2875	2893
2	1	627	607	618	648	660	618	609	647	609	611	640
2	p.a.	?	1040	1047	1040	1047	1047	--	--	--	--	
2	p.s.	?	1041	1048	1041	1048	1048	--	--	--	--	
2	2	?	1378	1395	1469	1489	1396	1385	1468	1386	1389	
2	3	?	1960	1983	2075	2103	1985	1967	2073	1969	1974	
2	4	?	2339	2366	2467	2502	2371					
3	1	787	773	783	803	815	796	773	802	786	786	832
3	2	1190	1137	1160	1203	1230	1166	1136	1197	1143	1145	1194
3	3	1602	1588	1619	1690	1726	1622	1587	1679	1589	1594	1650
4	1	1310	1307	1313	1348	1355	1371	1306	1346	1364	1359	1431
4	2	1503	1453	1475	1509	1535	1525	1450	1503	1501	1497	1575
4	3	1806	1714	1752	1797	1842	1788	1708	1784	1745	1744	1826
5	1	1938	1943	1949	2008	2014	2080	1941	2006	2073	2062	2253
5	2	2059	2020	2041	2088	2113	2163	2015	2080	2137	2126	2331
5	3	2276	2170	2214	2251	2304	2317	2159	2232	2262	2252	2474
6	1	2594	2567	2572	2673	2678	2770	2564	2668	2762	2750	3276
6	2	?	2606	2625	2707	2729	2798	2597	2691	2772	2762	
6	3	2802	2682	2724	2782	2833	2851	2663	2750	2800	2790	3424

[a]Tests performed by Hayek and Pallett.

[b]Gaps between segments of cylinder are "filled" by discrete rings with cross-section dimensions .33 x .375.

[c]Model A: Rotation and axial slippage permitted between end plates and cylinder.

[d]Model B: Axial slippage only permitted between end plates and cylinder.

[e]r.b. = "rigid body mode"

[f]p.a. = "plate antisymmetric" = end plates vibrating in phase.

[g]p.s. = "plate symmetric" = end plates vibrating out-of-plane.

[h]u = axial motion predominates.

SOME ASPECTS OF MODELING SHELLS

Some ideas about modeling have just been given. The purpose of this section is to give the user further hints about modeling for stress, buckling, and vibration analyses of practical shell of revolution.

Mesh Point Allocation

The analyst may wish to know what the stresses are in a shell at the bifurcation buckling load. If he sets up a single discretized model for both the stress and the buckling analyses, he must allocate nodal points such that stress concentrations as well as buckling modes can be predicted with reasonable accuracy. It is usually fairly easy to guess where the stress concentrations are, but more difficult to predict where the shell will buckle and the shape of the mode. Peak stresses can generally be predicted with enough accuracy if nodal points are spaced a few wall thicknesses apart. If a higher nodal point density is required for adequate convergence, thin shell theory may not represent a good enough model. Good estimates of buckling loads can usually be obtained with more than four nodal points per half wavelength of the buckling mode. Figure 23 depicts a ring stiffened cylinder which is submitted to external pressure. The prebuckling normal displacement and meridional moment and the buckling modal displacement distributions are also shown. Notice that mesh points are concentrated near the T-shaped rings and at the boundary where stress concentrations exist. Half the cylinder is modeled with symmetry conditions applied at the symmetry plane.

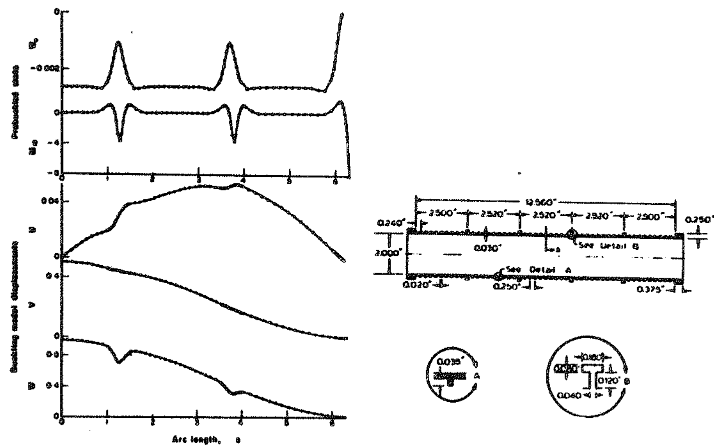

Fig. 23 Prebuckling state and buckling mode of an externally pressurized ring stiffened cylinder

Modeling Discrete Rings When Local Buckling Between Rings is Possible

Some BOSOR4 users have been concerned that occasionally buckling loads predicted for externally pressurized ring stiffened cylinders are unexpectedly high. In these cases the predicted buckling modes are usually local (deflections between rings with rings at nodes in the buckling pattern). Aside from the question of initial imperfections, there is another reason that too high buckling loads may be calculated: in the actual structure the webs of ring stiffeners probably deform considerably in the local buckling mode. This deformation can be accounted for if the webs of the rings are treated as flexible shell branches as shown in Fig. 24. The user should include in his parameter studies such a model, at least for a section of ring stiffened shell spanning two adjacent rings. It is rarely necessary to include the outstanding flanges as shells, since they can remain discrete rings.

Figure 25 shows a comparison of predicted buckling pressures of a cylinder with two models of a ring, one in which its cross section cannot deform (labeled "Ring") and the other in which it can (labeled "Branched Shell"). Reference [13] has more discussion on this and other points about modeling discrete rings.

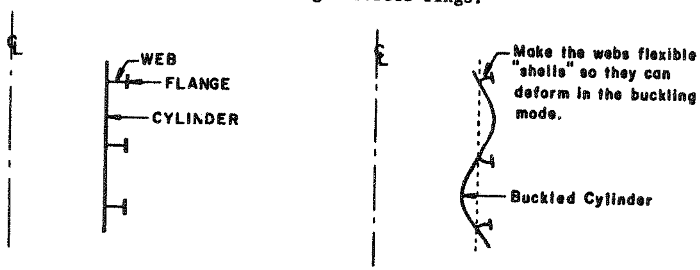

Fig. 24 Cylinder with ring webs modeled as flexible shell branches

When Stiffeners Can Be "Smeared"

If there exists a regular pattern of reasonably closely spaced stiffeners, their contribution to the wall stiffness of the shell or plate might be modeled by an averaging of their extensional and bending rigidities over arc lengths equal to the local spacings between them. Thus, the actual wall is treated as if it were orthotropic. In BOSOR4 this "smearing" process accounts for the fact that the neutral axes of the stiffeners do not in general lie in the plane of the reference surface of the shell wall. Predictions of buckling loads and vibration frequencies of stiffened cylinders have been found to be very sensitive to this eccentricity effect. A general rule of thumb for deciding to smear out the stiffeners or

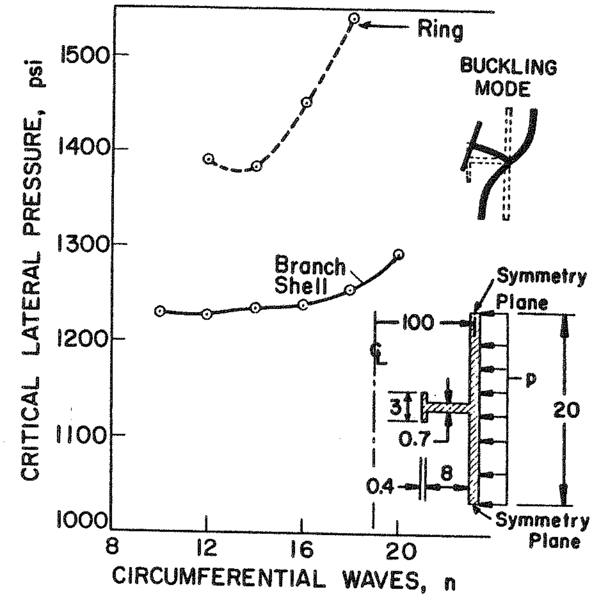

Fig. 25 Comparison of local buckling pressures of a ring stiffened cylinder for two models of the ring

to treat them as discrete is that for smearing there should be about 2 to 3 stiffeners per half wavelength of the deformation pattern. It may be appropriate to smear out stiffeners in a buckling or vibration analysis but, because of local stress concentrations caused by the stiffeners, not in a stress analyses. The stiffeners can be smeared as an analytical device to suppress local buckling and vibration modes. In order to handle problems involving smeared stiffeners, a computerized analysis must include coupling between bending and extensional energy.

Modeling Prismatic Shell Structures

An interesting and not immediately obvious use of BOSOR4 is for buckling and vibration analysis of prismatic shell structures, in particular composite branched panels. This technique of using a shell of revolution program for the treatment of structures that are not axisymmetric is discussed in detail in Ref [2]. Figure 26 shows various types of prismatic shell structures that can be handled by BOSOR4. Examples involving stress and buckling of oval cylinders, cylinders with nonuniform loads, and corrugated and beaded panels are given in Ref. [2], as well as a study of vibration of a stringer stiffened shell in which the stringers are treated as discrete. In the analysis of buckling of nonuniformly loaded cylinders, the nonsymmetry of the prestress can be accounted for in the stability analysis. In BOSOR4 the capability described in Ref. [2] is extended to branched prismatic shell structures.

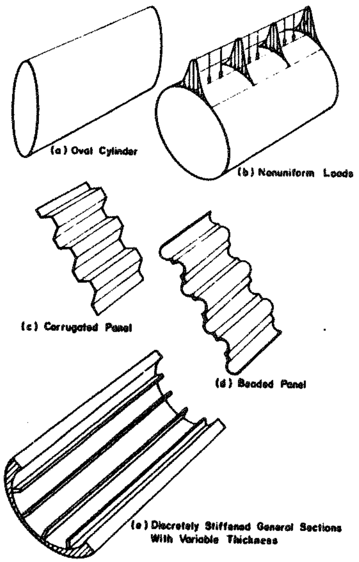

Fig. 26 Some prismatic shell structures that can be analyzed with use of BOSOR4

Example of Analysis of Prismatic "Shell" Structure

Figure 27 shows two types of semisandwich corrugated construction, bonded and riveted. The panels are treated as giant annuli with mean radius of 2,750 in. and outer radius minus inner radius equal to about 7.4 in. Both panels are assumed to carry an axial compressive stress (panels loaded normal to plane of figure) that is constant along the axis of the panel and over all of the little segments shown at the top of Fig. 27. In the model on the left-hand side of the figure the troughs of the corrugated sheet and the flat skin are assumed to be united by a perfect bond of zero thickness. The thickness of the panel in these areas is equal to the sum of the thickness of the flat sheet and the corrugated sheet. In the riveted panel the displacements and rotations of the corrugated sheet are constrained to be equal to those of the flat skin only at the midlengths of the troughs, thus simulating a rivet of zero diameter in the plane of the paper and continuous in the direction normal to the plane of the paper. The computer generated plots show the undeformed and deformed panels for buckling modes with various wave lengths L in the direction normal to the plane of the paper. The riveted panel is weaker in axial compression because the rivets permit more local distortion of the cross section than does the continuous bonding. The modes shown are more or less general instability modes. One can calculate buckling loads for much shorter L, such as L = 1.0 in., in order to determine the effect of fastening on crippling loads.

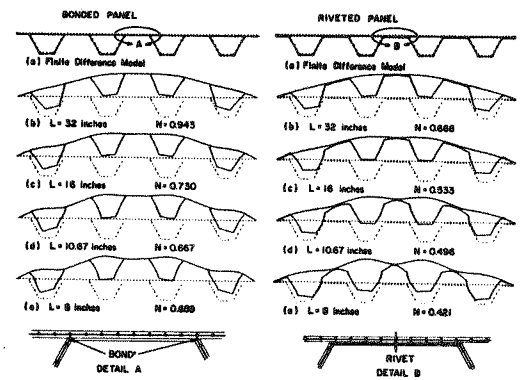

L = Axial Half-Wavelength of Buckling Mode.

$$N = \frac{\text{(Critical Axial Load)}}{\text{(Critical Axial Load With Local Distortion of Wall Cross-Section Not Allowed)}}$$

Fig. 27 Buckling modes and loads for axially compressed bonded and riveted corrugated panels

Modeling Concentrated Loads on Shells

The analyst may be interested in several types of concentrated loads which arise in various ways. If the shell structure is to be subjected to concentrated loads in the ordinary course of its service, such as a tank supported on struts or a rocket stage with discrete payload attach points, it is usually provided that the concentrated loads be applied to reinforced areas such as circumferential rings or longitudinal stringers through which these loads are smoothly diffused into the shell. Therefore, deflections are small, and a linear analysis is generally suitable. If, however, the analyst wants to find out what happens if the shell is accidentally poked somewhere, the concentrated load may be applied to an unreinforced area, and the shell may experience large deflections. Prediction of the effect of these accidental loads may therefore require nonlinear analysis. The point-loaded spherical cap, for which a load-deflection curve is shown in Fig. 15, is an example. In BOSOR4 a concentrated load applied such that nonsymmetric displacements occur is modeled as a line load with a triangular distribution around the circumference. Figure 28 shows an example. Each load is simulated by the area within the triangular "pulse" multiplied by some factor provided by the user as an input datum.

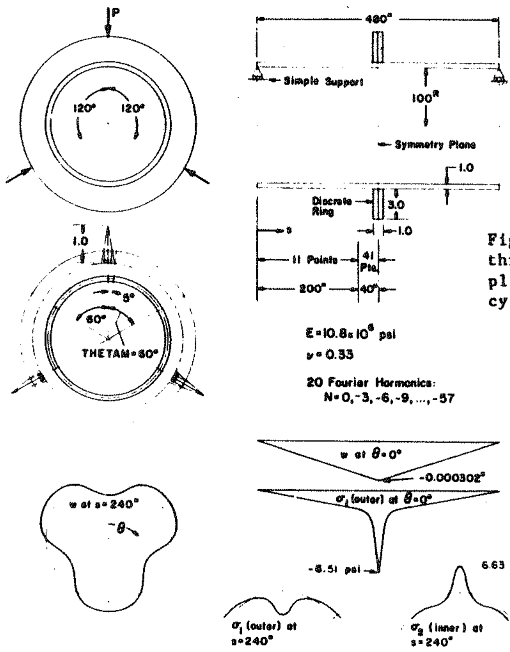

Fig. 28 Cylinder with three point loads applied to ring at cylinder midlength

Constraint Condition Problems to Be Wary Of

There are certain commonly occuring situations in which the program user should take great care with regard to constraint conditions. These involve rigid body behavior, symmetric vs. antisymmetric behavior at planes of symmetry in the structure, singularity conditions at poles of shells of revolution, discontinuities between various branches and segments of a complex shell structure, and unexpected sensitivity of predicted behavior to changes in boundary conditions.

Rigid body displacement. Rigid body displacement of an analytical model of a structure should not be permitted in static stress and buckling problems. In such problems the shell must be held in such a way that no constraints are introduced which are not actually present in the real structure. The proper application of rigid body constraint conditions requires special care in the case of nonsymmetrically loaded shells of revolution. These conditions apply only if the displacements are axisymmetric, or if the displacements vary with one circumferential wave around the circumference and must be released for higher displacement harmonics.

Symmetry planes. Many problems are best analyzed by a modeling of a small portion of the actual structure bounded by symmetry planes. In bifurcation buckling and modal vibration problems important modes may be antisymmetrical at one or more of the symmetry planes. This occurrence implies that symmetry boundary conditions should be applied in the prestress analysis and antisymmetry conditions at one or more of the symmetry planes in the eigenvalue analysis for bifurcation buckling or modal vibration. Unless the program user is certain about the behavior at a symmetry plane, he must make multiple runs on the computer, testing for both symmetrical and antisymmetrical behavior at each symmetry plane.

Singularity conditions at a pole. The problem of singularity conditions arises only in the case of shells of revolution or flat circular plates. As with rigid body modes, special conditions must be applied for axisymmetric ($n = 0$) displacements or for displacement modes with one circumferential wave ($n = 1$). If $n \geq 2$ the pole condition acts as a clamped boundary.

Constraint conditions for discontinuous domains. Practical shell structures are very frequently assembled so that the combined reference surfaces of the various branches and segments of the analytical model form a discontinuous domain. The BOSOR4 user should be aware that the constraint conditions governing the compatibility relations between adjacent surfaces imply that a rigid connection exists across the discontinuity. Thus the analytical model is stiffer than the actual structure. Buckling loads and vibration frequencies will be overestimated. It is likely that local discontinuity stresses will also be overestimated.

Unexpected sensitivity of predicted behavior to changes in boundary conditions. Frequently, complicated shell structures are designed and manufactured by more than one company or by more than one organization within a company. Each company or organization is responsible for only one particular segment of the entire structure, and often the properties of the adjoining segments are known only approximately if at all. Therefore some conditions must be assumed at the boundaries of each segment during the design phase of that segment. The purpose of this section is to warn the analyst that predictions of stress, buckling, and vibration of shells may be very sensitive to boundary conditions even though intuition dictates otherwise. Engineers interested in designing a particular segment of a larger structure should make every effort to determine as accurately as possible the actual boundary conditions at the ends of "their" segment. Portions of the adjoining segments should be included in the model, possibly with a cruder mesh. If little is known about the adjoining structures, sensitivity studies should be performed in which both upper and lower bounds on the degree of boundary constraint are assumed.

INPUT DATA

A preprocessor has been written for BOSOR4 by means of which the input data can be prepared in free format [14]. Figure 29 shows a sample BOSOR4 data deck.

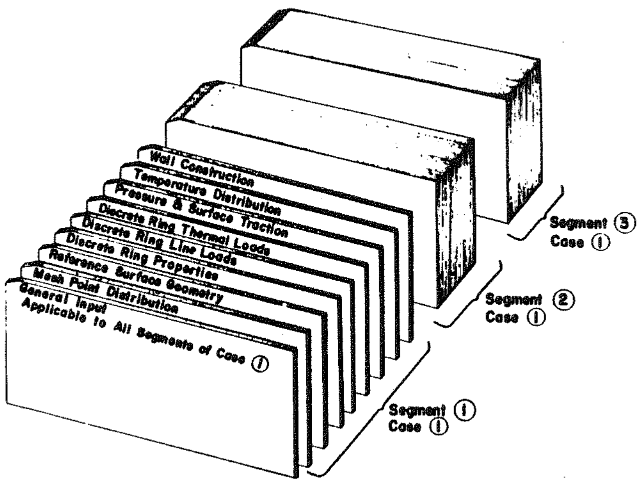

Fig. 29 Sample BOSOR4 data deck

ACKNOWLEDGEMENTS

The author is indebted to Frank Brogan, Tom Peterson, Chet Dyche, Bo Almroth, Bill Loden, and Rod Kure, who wrote some of the subroutines used in the BOSOR4 program. Particular appreciation is expressed for the many fruitful discussions with Frank Brogan and Bo Almroth concerning the numerical aspects of the analysis, and with Jörgen Skogh about ways in which to make the BOSOR4 program easy to use. The author is thankful also for Frank Brogan's assistance in the conversion of BOSOR4 for operation on the CDC 6600 and Tom Peterson's, Pete Smolenski's, and Bob Mitchell's assistance in the conversion for operation on the IBM 370/165.

The development of BOSOR4 was sponsored by the Department of Structural Mechanics of the Naval Ship Research and Development Center under Naval Ship Systems Command, Operation and Maintenance Navy Fund, Contract N00014-71-C-0002. Rembert Jones and Joan Roderick were technical monitors. The work involved in converting BOSOR4 for operation on the CDC 6600 was sponsored by the NASA Langley Research Center, Contract NAS1-10929, with Paul Cooper as technical monitor

Some of the numerical studies were performed under the Lockheed Missiles & Space Company's Independent Research Program. The support of ONR under Contract N00014-76-C-0692, with Nicholas Perrone and Kenneth Saczalski as technical monitors, is gratefully acknowledged.

The following figures have been reprinted by permission:

Figs. 1 - 3 from D. Bushnell, B. O. Almroth, and F. Brogan, "Finite-Diference Energy Method for Nonlinear Shell Analysis," Computers & Structures, Vol. 1, 1971, pp. 361-387, © 1971.

Figs. 7, 8, 11, 12, 14, 19, 20, 28, 29 and Table 2 from D. Bushnell, "Stress, Stability and Vibration of Complex, Branched Shells of Revolution," Computers & Structures, Vol. 4, 1974, pp. 399-435, © 1974.

Figs. 9, 10 from D. Bushnell, "Finite-Difference Energy Models versus Finite-Element Models: Two Variational Approaches in One Computer Program," Numerical and Computer Methods in Structural Mechanics, pp. 291-336, © 1973, Academic Press, New York.

Fig. 13 from D. Bushnell, "Nonlinear Analysis for Axisymmetric Elastic Stresses in Ring-Stiffened, Segmented Shells of Revolution," AIAA/ASME 10th Structures, Structural Dynamics and Materials Conference, pp. 104-113, © 1969, ASME.

Fig. 16, 17 from D. Bushnell, "Crippling and Buckling of Corrugated Ring-Stiffened Cylinders," AIAA Journal of Spacecraft and Rockets, Vol. 9, No. 5, 1972, pp. 357-363, © 1972, AIAA.

Fig. 18 from D. Bushnell and S. Smith, "Stress and Buckling of Nonuniformly Heated Cylindrical and Conical Shells," AIAA Journal, Vol. 9, No. 12, Dec. 1971, pp. 2314-2321, © 1971, AIAA.

Figs. 21 through 23 and Table 3 from D. Bushnell, "Thin Shells," Structural Mechanics Computer Programs, University Press of Virginia, pp. 277-358 © 1972.

Fig. 26 from D. Bushnell, "Stress, Buckling, and Vibration of Prismatic Shells," AIAA Journal, Vol 9, No. 10, Oct. 1971, pp. 2003-2013, © 1971, AIAA.

Fig. 27 from D. Bushnell, "Evaluation of Various Analytical Models for Buckling and Vibration of Stiffened Shells," AIAA Journal, Vol. 11, No. 9, 1973, pp. 1283-1291 © 1973, AIAA.

REFERENCES

1 Bushnell, D., "Stress, Stability, and Vibration of Complex Branched Shells of Revolution, Analysis and User's Manual for BOSOR4," LMSC-D243605, Lockheed Missiles & Space Co., Inc., Sunnyvale, Ca., March 1972.
Also NASA CR-2116, Oct. 1972.

2 Bushnell, D., "Stress, Buckling, and Vibration of Prismatic Shells," AIAA Journal, Vol. 9, No. 10, Oct. 1971, pp. 2004-13.

3 Bushnell, D., Almroth, B. O., and Brogan, F. A., "Finite-Difference Energy Method for Nonlinear Shell Analysis," Journal for Computers & Structures, Vol. 1, 1971, pp. 361-87.

4 Bushnell, D., "Analysis of Ring-Stiffened Shells of Revolution under Combined Thermal and Mechanical Loading," AIAA Journal, Vol. 9, No. 3, March 1971, pp. 401-10.

5 Bushnell, D., "Finite-Difference Energy Models Versus Finite Element Models: Two Variational Approaches in One Computer Program," Numerical and Computer Methods in Structural Mechanics, edited by Fenves, S. J., Perrone, N., Robinson, A. R., and Schnobrich, W. C., Academic Press, Inc., New York and London, 1973, pp. 291-336.

6 Bushnell, D., "Analysis of Buckling and Vibration of Ring-Stiffened, Segmented Shells of Revolution," International Journal of Solids Structures, Vol. 6, 1970, pp. 157-181.

7 Bushnell, D., "Thin Shells," Structural Mechanics Computer Programs, edited by Pilkey, W., Saczalski, K. and Schaeffer, H., University Press of Virginia, Charlottesville, 1974, pp. 277-358.

8 Penning, F. A. and Thurston, G. A., "The Stability of Shallow Spherical Shells Under Concentrated Load," NASA CR-265, July 1965.

9 Holmes, A., "Measurement of Thermal Stresses in Ring-Stiffened Cylinders," LMSC-Y1-69-66-1, Lockheed Missiles & Space Co., Palo Alto, Ca., Dec. 1966.

10 Bushnell, D. and Smith, S., "Stress and Buckling of Nonuniformly Heated Cylindrical and Conical Shells," AIAA Journal, Vol. 9, No. 12, 1971, pp. 2314-2321.

11 Hayek, S. and Pallett, D. S., "Theoretical and Experimental Studies of the Vibration of Fluid Loaded Cylindrical Shells," Symposium on Application of Experimental and Theoretical Structural Dynamics, Southampton University, England, April 1972.

12 Harari, A. and Baron, M. L., "Analysis for the Dynamic Response of Stiffened Shells," ASME Paper No. 73-APM-FFF, to appear J. Appl. Mech.

13 Bushnell, D., "Evaluation of Various Analytical Models for Buckling and Vibration of Stiffened Shells," AIAA Journal, Vol. 11, No. 9, 1973, pp. 1283-1291.

14 BOSOR4 PREPROCESSOR written by and available from SKD Enterprise, 9138 Barberry Lane, Hickory Hills, Illinois 60457.

APPENDIX A

BOSOR4 INPUT DATA

This appendix is organized in the following way: First there is a page which gives some useful hints on how to set up a case; then there are two pages which define certain input data that depend on what type of analysis is to be performed; these two pages are followed by seven pages describing constraint and juncture conditions; then come three pages on load and temperature multipliers and ranges. All of these pages just described correspond to the initial cards in the input deck labeled "General Input--Applicable to All Segments of Case 1" in Fig. 29.

The remaining input data for a case are defined on pages 61 - 98. These data are required for each segment of the structure. The data input section is subdivided into the following subsections:

1. Mesh Point Distribution
2. Reference Surface Geometry
3. Discrete Ring Properties
4. Discrete Ring Line Loads
5. Discrete Ring Thermal Loads
6. Pressure and Surface Traction
7. Temperature Distribution
8. Prestress Input Data for the Option INDI = 4, IPRE = 0
9. Wall Construction

The input data specifications are written in a style very similar to FORTRAN. It is therefore assumed that the user is familiar with this language.

Following the input data definition are sample input decks corresponding to each type of analysis. (INDIC = 1, -1, 0, 2, 3, 4, -2). The user is urged to consult these cases since they will clarify many of the input specifications which may at first seem rather arcane.

A section entitled "Possible Pitfalls and Recommended Solutions" then follows. The user should read this section even if he has not yet encountered a problem. There are some suggestions given there that may help the user decide how to set up an appropriate model.

Finally, there is a brief description of BOSOR4 output, including sample list and plot output corresponding to the first sample case.